

MAIDESC M30 :AGENDA



09:00 Accueil

10:00-10:40 Cemef : ???

10:40-11:20 Rocquencourt: Norm oriented en CFD (Loic Frazza)

11:20-12:00 Transvalor : Fully automatic meshing process for complex structures to capture fluid-structure efforts (Alexandre Boilley).

12:00-12:40 Lemma : Métriques discrètes (G. Brethes, INRIA-Lemma, A. Dervieux, INRIA-Lemma)

13:00-14:00 Repas

14:00-14:40 Sophia : Adaptation ALE: théorie (E. Gauci, A. Dervieux)

14:40-15:20 Montpellier : A Volume-agglomeration multirate advancing approach (Emmanuelle Itam)

15:20-16:00 Table ronde



MAIDESC

Contribution Lemma à Maidesc (M30)

Gautier Brethes^{*+}, Olivier Allain^{*}, Alain Dervieux^{*+}

(^{*}) Lemma, , Sophia-Antipolis, France

(⁺) INRIA, , Sophia-Antipolis, France

April 12, 2016

Overview

Proposal

T4-D6: Interface meshing for unsteady simulations (M18,M30).

T5-D4: Extension of Adaptive FMG to the unsteady simulation of two-phase flows (M42).

Test cases: Dam break (ITC1) et capillarité dans un réservoir (ITC2).

Task status

T4-D6: M18 delivered with the new method (ITC1). Next version : M36.

T4-D6: New version of discrete capillarity (ITC2).

T5-D4: Parallel FMG for CFD, in progress.

T5-D4: **Adaptive FMG: investigation of tensorial criteria.**

Adaptive FMG: investigation of tensorial criteria

Recalls on continuous metrics

Integrals over a discrete mesh

Second-order metric: Hessian

Second-order metric: goal-oriented

Second-order metric: norm-oriented

Optimal metric

Numerical examples

Recalls : continuous (implicit) metric

$$\mathcal{M} = \mathcal{R} \begin{pmatrix} h_1^{-2} & 0 & 0 \\ 0 & h_2^{-2} & 0 \\ 0 & 0 & h_3^{-2} \end{pmatrix} {}^t \mathcal{R}$$

Mesure locale de cellule:

$$h_1 h_2 h_3 = (\det(\mathcal{M}))^{-\frac{1}{2}}.$$

Densite locale de points:

$$d = (h_1 h_2 h_3)^{-1} \Rightarrow C(\mathcal{M}) = \int_{\Omega} \sqrt{\det(\mathcal{M})} dv$$

$$\ell_{\mathcal{M}}(\mathbf{e}_i) = \int_0^1 \sqrt{{}^t \mathbf{a} \mathbf{b} \mathcal{M} (\mathbf{a} + t \mathbf{a} \mathbf{b}) \mathbf{a} \mathbf{b}} dt, \text{ with } \mathbf{e}_i = \mathbf{a} \mathbf{b}.$$

Unit mesh $\mathbf{x}_{ij}^{\mathcal{M}}$: its edges $\mathbf{x}_{ij}^{\mathcal{M}}$ satisfy:

$$\ell_{\mathcal{M}}(\mathbf{x}_{ij}) = 1 \Leftrightarrow (\mathbf{x}_{ij}^{\mathcal{M}}, \mathcal{M} \mathbf{x}_{ij}^{\mathcal{M}}) = 1 \quad \forall (i,j) \text{ neighboring vertices.}$$

Recalls : optimal continuous metric, iso/Lp

Optimal continuous metric minimizing the interpolation error:

$$\text{Min}|u - \Pi_{\mathcal{M}}u|_{L^\infty}, \quad \text{Min}|u - \Pi_{\mathcal{M}}u|_{L^p}$$

$$|u - \Pi_{\mathcal{M}}u| \approx \frac{1}{8} |\text{tr}(\mathcal{M}^{-\frac{1}{2}} |H_u| \mathcal{M}^{-\frac{1}{2}})|$$

H_u Hessian of u .

Pointwise optimization: For both norms, *same level of error in each direction* around a given point i of the computational domain (Loseille-Alauzet, SIAM 2011).

$$\mathcal{M}_{opt}^i = m_i |H_u^i| \quad \forall i \in \Omega.$$

The global optimization determines m_i :

$$\mathcal{M}_{L^\infty} = N^{\frac{2}{3}} \left(\int \det(|H_u|) \right)^{-\frac{2}{3}} |H_u|$$

$$\mathcal{M}_{L^1} = N^{\frac{2}{3}} \left(\int \det(|H_u|)^{\frac{2}{3}} \right)^{-\frac{2}{3}} \det(|H_u|)^{-\frac{1}{3}} |H_u|$$

Integral on a given mesh (1)

Given a mesh \mathbf{x}_{ij} , we can define the following partitions:

- a *mesh-vertex* is a vertex of an element of the mesh.
- *elements* : triangles or tetrahedra.

Elements are divided in *sub-elements*.

Sub-elements: 6 *subtriangles* using medians and 24 *subtetrahedra* using median plans. The vertices of a subtetrahedron are : a mesh-vertex i , a center I_{ij} of an edge ij having i as extremity, the centroid g_{ijk} of a face ijk containing i and j , the element centroid G_{ijkl} . The measure of a subtetrahedron of the tetrahedron T is $1/24 \text{ meas}(T)$.

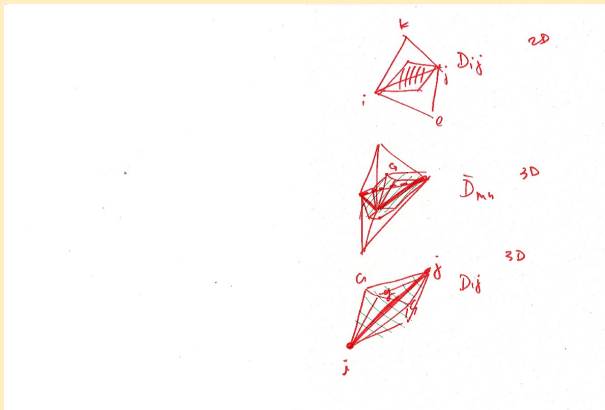
- *Cell i* : for a vertex i of the mesh, cell i is union of sub-elements having i as vertex of the sub-element. A cell measure is defined as

$$\text{meas}_{\mathbf{x}}(i) = \frac{1}{\text{dim}+1} \sum_{T_{\mathbf{x}} \ni i} \text{meas}(T_{\mathbf{x}})$$

where $T_{\mathbf{x}}$ are elements of \mathbf{x} containing i .

Integral on a given mesh (2)

- *2D-diamond* D_{ij} : union of the 4 subtriangles (of triangles ijk and ijl) having a side beared by edge ij .
- *face-diamond* \bar{D}_{mn} , where m and n are two tetrahedra having a common face ijk : union of 6 subtetrahedra having a subtriangle of the common face ijk as face.
- *edge-diamond* D_{ij} : union of subtetrahedra having having a side beared by edge ij .



Integral on a given mesh (3)

The integral of a function e_{ij} defined on the edges can be approximated by:

$$err_{L^1} = \sum_i meas_{\mathbf{x}}(i) \Gamma(i)^{-1} \sum_j e_{ij}$$

or introducing the diamond partition $\Omega = \cup \bar{D}_{mn}$ where m and n are elements with a common face:

$$err_{L^1} = \frac{1}{3} \sum_{\bar{D}_{mn}} meas_{\mathbf{x}}(\bar{D}_{mn}) (e_{ij} + e_{ik} + e_{jk}).$$

where i, j, k are vertices of the face mn .

Discretizing an arbitrary continuous metric on a given mesh

Assume that the metric \mathcal{M} is defined on the vertices $\mathcal{M}(\mathbf{x}_i) = \mathcal{M}^i$ of the given mesh and P^1 -continuously interpolated. The total number of nodes of N can be approximated on the mesh \mathbf{x} as follows:

$$N = \sum_i \text{meas}_{\mathbf{x}}(i) \sqrt{\det(\mathcal{M}^i)}$$

To simplify, we assume that the unit mesh is a deformation of \mathbf{x} , and that $\mathbf{x}_{ij}^{\mathcal{M}}$ and \mathbf{x}_{ij} are colinear.

Then the lengths are related by:

$$\begin{aligned} (\mathbf{x}_{ij}^{\mathcal{M}}, \mathcal{M} \mathbf{x}_{ij}^{\mathcal{M}}) = 1 &= \left(\mathbf{x}_{ij} \frac{|\mathbf{x}_{ij}^{\mathcal{M}}|}{|\mathbf{x}_{ij}|}, \mathcal{M} \mathbf{x}_{ij} \frac{|\mathbf{x}_{ij}^{\mathcal{M}}|}{|\mathbf{x}_{ij}|} \right) = (\mathbf{x}_{ij}, \mathcal{M} \mathbf{x}_{ij}) \frac{|\mathbf{x}_{ij}^{\mathcal{M}}|^2}{|\mathbf{x}_{ij}|^2} \\ \Rightarrow \mathbf{x}_{ij}^{\mathcal{M}} &\approx \mathbf{x}_{ij} (\mathbf{x}_{ij}, \mathcal{M} \mathbf{x}_{ij})^{-\frac{1}{2}} \end{aligned}$$

Second-order error of a metric on another mesh

We want to evaluate on mesh \mathbf{x} a directional quadratic error $e_{ij}^{\mathcal{M}} = \bar{e}_{ij} |\mathbf{x}_{ij}^{\mathcal{M}}|^2$ produced by the unit mesh $\mathbf{x}^{\mathcal{M}}$. We assume that \bar{e}_{ij} depends only on location and direction of $\mathbf{x}_{ij}^{\mathcal{M}}$, typically:

$$e_{ij}^{\mathcal{M}} = |\mathbf{x}_{ij}^{\mathcal{M}}|^2 \bar{e}_{ij}\left(\frac{1}{2}(\mathbf{x}_i^{\mathcal{M}} + \mathbf{x}_j^{\mathcal{M}}), \frac{\mathbf{x}_{ij}^{\mathcal{M}}}{|\mathbf{x}_{ij}^{\mathcal{M}}|}\right).$$

To evaluate this error on the initial mesh \mathbf{x} , we assume that the unit mesh is a deformation of \mathbf{x} in such a way that $\mathbf{x}_{ij}^{\mathcal{M}}$ and \mathbf{x}_{ij} are colinear.

Then the intensity $e_{ij}^{\mathcal{M}}$ of the error with the unit mesh evaluated at middle of \mathbf{x}_{ij} of the initial mesh writes:

$$e_{ij}^{\mathcal{M}} = |\mathbf{x}_{ij}|^2 (\mathbf{x}_{ij}, \mathcal{M}_{ij}\mathbf{x}_{ij})^{-1} \bar{e}_{ij}\left(\frac{1}{2}(\mathbf{x}_i + \mathbf{x}_j), \frac{\mathbf{x}_{ij}}{|\mathbf{x}_{ij}|}\right)$$

where \mathcal{M}_{ij} is evaluated on $\frac{1}{2}(\mathbf{x}_i + \mathbf{x}_j)$.

First example of second-order error: HESSIAN

Hessian with weight g

The intensity of interpolation error of a quadratic function u on $\mathbf{x}_{ij}^{\mathcal{M}}$ writes:

$$\int |g| |u - \Pi_h u| d\Omega \preceq \sum_i \text{meas}_{\mathbf{x}}(i) \Gamma(i)^{-1} \sum_j e_{ij}^{\mathcal{M},g,u}(\mathbf{x}_{ij})$$

$$e_{ij}^{\mathcal{M},g,u} = |\mathbf{x}_{ij}^{\mathcal{M}}|^2 |g_{ij}| |H_{ij}| \cdot \frac{\mathbf{x}_{ij}^{\mathcal{M}}}{|\mathbf{x}_{ij}^{\mathcal{M}}|} \cdot \frac{\mathbf{x}_{ij}^{\mathcal{M}}}{|\mathbf{x}_{ij}^{\mathcal{M}}|}.$$

where $H_{ij} = H(\frac{1}{2}(\mathbf{x}_i^{\mathcal{M}} + \mathbf{x}_j^{\mathcal{M}}))$, $H(\mathbf{x})$ being the Hessian of u at point \mathbf{x} , and $g_{ij} = g(\frac{1}{2}(\mathbf{x}_i^{\mathcal{M}} + \mathbf{x}_j^{\mathcal{M}}))$. In practice, it is evaluated on the initial mesh:

$$e_{ij}^{\mathcal{M},g,u}(\mathbf{x}_{ij}) = |\mathbf{x}_{ij}^{\mathcal{M}}|^2 \quad \bar{e}_{ij}(\mathbf{x}_{ij}) = (\mathbf{x}_{ij}, \mathcal{M} \mathbf{x}_{ij})^{-1} |\mathbf{x}_{ij}|^2 \quad \bar{e}_{ij}(\mathbf{x}_{ij})$$

with:

$$\bar{e}_{ij}(\mathbf{x}_{ij}) = |g_{ij}(\mathbf{x}_{ij})| |H_{ij}(\mathbf{x}_{ij})| \cdot \frac{\mathbf{x}_{ij}^{\mathcal{M}}}{|\mathbf{x}_{ij}^{\mathcal{M}}|} \cdot \frac{\mathbf{x}_{ij}^{\mathcal{M}}}{|\mathbf{x}_{ij}^{\mathcal{M}}|} = |g_{ij}(\mathbf{x}_{ij})| |H_{ij}(\mathbf{x}_{ij})| \cdot \frac{\mathbf{x}_{ij}}{|\mathbf{x}_{ij}|} \cdot \frac{\mathbf{x}_{ij}}{|\mathbf{x}_{ij}|}.$$

Second example of second-order error: GOAL (1)

Goal-oriented 3D

Quadratic errors can also be encountered in the case of a goal-oriented error analysis. Let u be the solution of the EDP and $u_{\mathcal{M}}$ the solution of the discretized EDP when the mesh is an unit mesh for metric \mathcal{M} . A typical goal-oriented analysis relies on the minimization of the error $\delta j_{goal}(\mathcal{M})$ done in the evaluation of the scalar output $j = (g, u)$, error which we write as follows:

$$\delta j_{goal}(\mathcal{M}) = |(g, u - u_{\mathcal{M}})| = |(g, \Pi_{\mathcal{M}}u - u_{\mathcal{M}} + u - \Pi_{\mathcal{M}}u)|. \quad (1)$$

According to the Aubin-Nitsche analysis, this error is second-order with respect to mesh size. Let us define the discrete adjoint state u_{goal}^* :

$$\forall \psi_{\mathcal{M}} \in V_{\mathcal{M}}, \quad a(\psi_{\mathcal{M}}, u_{goal}^*) = (\psi_{\mathcal{M}}, g). \quad (2)$$

In the sequel, we use a fixed-point in which the adjoint is frozen with respect to the metric \mathcal{M} . Injecting (5) in (4) we get:

$$(g, \Pi_{\mathcal{M}}u - u_{\mathcal{M}} + u - \Pi_{\mathcal{M}}u) = a(\Pi_{\mathcal{M}}u - u_{\mathcal{M}}, u_{goal}^*) + (g, u - \Pi_{\mathcal{M}}u)$$

Second example of second-order error: GOAL (2)

Goal-oriented 3D

and, using *a priori* estimation,

$$(g, \Pi_{\mathcal{M}}u - u_{\mathcal{M}} + u - \Pi_{\mathcal{M}}u) = a(\Pi_{\mathcal{M}}u - u, u_{goal}^*) + (f - \Pi_{\mathcal{M}}f, u_{goal}^*) + (g, u - \Pi_{\mathcal{M}}u)$$

thus

$$\delta j_{goal}(\mathcal{M}) \approx |a(\Pi_{\mathcal{M}}u - u, u_{goal}^*) + (f - \Pi_{\mathcal{M}}f, u_{goal}^*) + (g, u - \Pi_{\mathcal{M}}u)|$$

Recall that u is unknown. The second and third terms, similar to the main term of the Hessian-based adaptation in previous section can be explicitly approached in the same way.

$$\delta j_{goal}(\mathcal{M}) \preceq |a(\Pi_{\mathcal{M}}u - u, u_{goal}^*)| + |(f - \Pi_{\mathcal{M}}f, u_{goal}^*)| + |g||u - \Pi_{\mathcal{M}}u|$$

Second example of second-order error: GOAL (3)

Goal-oriented 3D

The second and third terms give Hessian-like quadratic errors $e_{ij}^{\mathcal{M}, u^*_{goal}, f}$ and $e_{ij}^{\mathcal{M}, g, u}$:

$$\begin{aligned} & |(f - \Pi_{\mathcal{M}} f, u^*_{goal})| + |g| |\pi_{\mathcal{M}} u_{\mathcal{M}} - u_{\mathcal{M}}| \\ & \leq \sum_i meas_{\mathbf{x}}(i) \Gamma(i)^{-1} \sum_{ij \ni i} \left(e_{ij}^{\mathcal{M}, u^*_{goal}, f} + e_{ij}^{\mathcal{M}, g, u} \right) \\ & \leq \sum_i meas_{\mathbf{x}}(i) \Gamma(i)^{-1} \sum_{ij \ni i} (\mathbf{x}_{ij}, \mathcal{M} \mathbf{x}_{ij})^{-1} |\mathbf{x}_{ij}|^2 \left(\bar{e}_{ij}^{u^*_{goal}, f} + \bar{e}_{ij}^{g, u} \right) \end{aligned}$$

with

$$\bar{e}_{ij}^{u^*_{goal}, f}(\mathbf{x}_{ij}) = |u^*_{goal, ij}| |H_{ij}^f| \cdot \frac{\mathbf{x}_{ij}}{|\mathbf{x}_{ij}|} \cdot \frac{\mathbf{x}_{ij}}{|\mathbf{x}_{ij}|} \quad ; \quad u^*_{goal, ij} = u^*_{goal} \left(\frac{\mathbf{x}_i + \mathbf{x}_j}{2} \right)$$

$$\bar{e}_{ij}^{g, u}(\mathbf{x}_{ij}) = |g_{ij}| |H_{ij}^u| \cdot \frac{\mathbf{x}_{ij}}{|\mathbf{x}_{ij}|} \cdot \frac{\mathbf{x}_{ij}}{|\mathbf{x}_{ij}|} \quad ; \quad g_{ij} = g \left(\frac{\mathbf{x}_i + \mathbf{x}_j}{2} \right)$$

and

$$H_{ij}^f = H^f \left(\frac{\mathbf{x}_i + \mathbf{x}_j}{2} \right) \quad ; \quad H_{ij}^u = H^u \left(\frac{\mathbf{x}_i + \mathbf{x}_j}{2} \right).$$

Second example of second-order error: GOAL (4)

Goal-oriented 3D

The first term is more complex. It can be estimated in a different way from the continuous method presented in Belme's PHD and used in Brethes's second paper.

$$\left| \int_{\Omega} \nabla(\Pi_{\mathcal{M}}u - u) \nabla \Pi_{\mathcal{M}}u_{goal}^* \, d\mathbf{x} \right| \preceq \sum_{\partial T_{mn}} |\nabla u_{goal}^*|_{T_m} - \nabla u_{goal}^*|_{T_n} \cdot \mathbf{n}_{mn} \int_{\partial T_{mn}} |\Pi_{\mathcal{M}}u - u| \, d\sigma.$$

In the 3D case, the intersection ∂T_{mn} of two elements T_m and T_n is a common face with vertices i, j, k and an area $area(mn)$. The following quantity is known:

$$\kappa_{mn}(u_{goal}^*) = \left| [(\nabla u_{goal}^*)|_{T_m} \cdot \mathbf{n}_{mn} - (\nabla u_{goal}^*)|_{T_n} \cdot \mathbf{n}_{mn}] \right|.$$

The remaining expression can be expressed in terms of interpolation errors:

$$\int_{\partial T_{mn}} |\Pi_{\mathcal{M}}u - u| \approx \frac{1}{3} area(mn) (e_{ij}^{\mathcal{M},u} + e_{ik}^{\mathcal{M},u} + e_{kj}^{\mathcal{M},u})$$

with (for $\alpha\beta=ij, ik$ and kj):

$$e_{\alpha\beta}^{\mathcal{M},u} = (\mathbf{x}_{\alpha\beta}, \mathcal{M} \mathbf{x}_{\alpha\beta})^{-1} |\mathbf{x}_{\alpha\beta}|^2 \bar{e}_{\alpha\beta}^u$$

Second example of second-order error: GOAL (5)

Goal-oriented 3D

$$e_{\alpha\beta}^{-\bar{u}}(\mathbf{x}_{\alpha\beta}) = |g_{\alpha\beta}| |H_{\alpha\beta}^u| \cdot \frac{\mathbf{x}_{\alpha\beta}}{|\mathbf{x}_{\alpha\beta}|} \cdot \frac{\mathbf{x}_{\alpha\beta}}{|\mathbf{x}_{\alpha\beta}|}.$$

We get:

$$|a(\Pi_{\mathcal{M}}u - u, u_{goal}^*)| \leq \sum_{\bar{D}_{mn}} |\bar{D}_{mn}| \frac{area(mn)}{|\bar{D}_{mn}|} \frac{1}{3} (e_{ij}^{\mathcal{M},u} + e_{ik}^{\mathcal{M},u} + e_{jk}^{\mathcal{M},u}) \kappa_{mn}(u_{goal}^*)$$

Let us convert the RHS into an edge-by-edge sum:

$$\begin{aligned} |a(\Pi_{\mathcal{M}}u - u, u_{goal}^*)| &\leq \sum_{\bar{D}_{mn}} \sum_{\alpha\beta=ij,ik,jk} area(mn) \frac{1}{3} e_{\alpha\beta}^{\mathcal{M}} \kappa_{mn}(u_{goal}^*) \\ &= \sum_{\text{edges } ij} \sum_{\bar{D}_{mn} \ni ij} area(mn) \frac{1}{3} e_{ij}^{\mathcal{M}} \kappa_{mn}(u_{goal}^*) = \sum_{\text{edges } ij} e_{ij}^{\mathcal{M},a} |D_{ij}| \end{aligned}$$

Second example of second-order error: GOAL (6)

Goal-oriented 3D

where we recognize the edge-by-edge integral of a field $e_{ij}^{\mathcal{M},a}$ defined on edges, with the notation:

$$e_{ij}^{\mathcal{M},a} = \frac{1}{|D_{ij}|} \sum_{\bar{D}_{mn} \ni ij} \text{area}(mn) \frac{1}{3} e_{ij}^{\mathcal{M}} \kappa_{mn}(u_{goal}^*). \quad (3)$$

Equivalently (at the second order) we get the previous error format:

$$|a(\Pi_{\mathcal{M}} u - u, u_{goal}^*)| \preceq \sum_i \text{meas}_{\mathbf{x}}(i) \frac{1}{\Gamma(i)} \sum_{ij \ni i} e_{ij}^{\mathcal{M},a}.$$

Gathering the analyses of the three terms, introducing:

$$\bar{e}_{ij}^{\mathcal{M},a} = (\mathbf{x}_{ij}, \mathcal{M} \mathbf{x}_{ij}) |\mathbf{x}_{ij}|^{-2} e_{ij}^{\mathcal{M},a}$$

we get:

$$\delta j_{goal}(\mathcal{M}) \preceq \sum_i \text{meas}_{\mathbf{x}}(i) \Gamma(i)^{-1} \sum_{ij \ni i} (\mathbf{x}_{ij}, \mathcal{M} \mathbf{x}_{ij})^{-1} |\mathbf{x}_{ij}|^2 \left(\bar{e}_{ij}^{\mathcal{M},a} + \bar{e}_{ij}^{u_{goal}^*,f} + \bar{e}_{ij}^{g,u} \right)$$

Third example of second-order error: NORM (1)

Norm-oriented

Quadratic errors can also be encountered in the case of a norm-oriented error analysis.

$$\delta j_{norm}(\mathcal{M}) = |(u'_{\mathcal{M}}, u - u_{\mathcal{M}})| = |(u'_{\mathcal{M}}, \Pi_{\mathcal{M}}u - u_{\mathcal{M}} + u - \Pi_{\mathcal{M}}u)|. \quad (4)$$

Where $u'_{\mathcal{M}}$ is any corrector approaching the difference $u - u_{\mathcal{M}}$. Let us define the discrete adjoint state u_{norm}^* :

$$\forall \psi_{\mathcal{M}} \in V_{\mathcal{M}}, \quad a(\psi_{\mathcal{M}}, u_{norm}^*) = (\psi_{\mathcal{M}}, u'_{\mathcal{M}}). \quad (5)$$

The rest of the method follows the lines of the goal method.

The main interest is that the new formulation is focused on the L^2 convergence of the approximation, while the goal-oriented formulation guarantees only the convergence of the chosen output.

Discretizing an arbitrary continuous metric on a given mesh (2)

For any of the three above error type, the intensity of error on mesh $\tilde{\mathbf{x}}$ unit for \mathcal{M} can be evaluated on \mathbf{x}_{ij} :

$$e_{ij}^{\mathcal{M}} = (\mathbf{x}_{ij})^2 (\mathbf{x}_{ij}, \mathcal{M} \mathbf{x}_{ij})^{-1} \bar{e}_{ij}$$

The integral of it can be approximated by:

$$err_{L^1} = \sum_i meas_{\mathbf{x}}(i) \Gamma(i)^{-1} \sum_{\mathbf{x}_{ij}} (\mathbf{x}_{ij})^2 (\mathbf{x}_{ij}, \mathcal{M} \mathbf{x}_{ij})^{-1} \bar{e}_{ij}$$

The purpose is to minimize with respect to the metric for a given number of vertices.

Pointwise optimal metric

The purpose of the *pointwise metric optimisation* is to look for the optimal stretching of the metric in any vertex, independantly of the global mesh density. The number of vertices is fixed. We consider metric \mathcal{M}_0 such that the determinant, or product of eigenvalues is equal to unity, i.e. $\lambda_1 \lambda_2 \lambda_3 = 1$ or, equivalently $\det(\mathcal{M}_0) = 1$. We know that:

$$(\mathbf{x}_{ij})^2 (\mathbf{x}_{ij}, \mathcal{M} \mathbf{x}_{ij})^{-1} \bar{e}_{ij} = e_{ij}^{\mathcal{M}} \quad \forall j.$$

In that expression, $(\mathbf{x}_{ij})^2$ and $(\mathbf{x}_{ij}, \mathcal{M} \mathbf{x}_{ij})^{-1}$ are not vanishing for any couple of neighboring vertices i and j , which implies

$$e_{ij}^{\mathcal{M}} = 0 \Leftrightarrow \bar{e}_{ij} = 0.$$

Now, for any i and any j belonging to $\Gamma(i)$ such that $\bar{e}_{ij} \neq 0$,

$$(\mathbf{x}_{ij})^{-2} (\mathbf{x}_{ij}, \mathcal{M} \mathbf{x}_{ij}) (\bar{e}_{ij})^{-1} = (e_{ij}^{\mathcal{M}})^{-1}.$$

Pointwise optimal metric(2)

Summing around the vertex i , it gives:

$$\sum_{\substack{j \in \Gamma(i) \\ |\bar{e}_{ij} \neq 0}} (\mathbf{x}_{ij})^{-2} (\bar{e}_{ij})^{-1} (\mathbf{x}_{ij}, \mathcal{M} \mathbf{x}_{ij}) = \sum_{\substack{j \in \Gamma(i) \\ |\bar{e}_{ij} \neq 0}} (e_{ij}^{\mathcal{M}})^{-1}$$

For the sake of simplicity, let us denote: $D_i = \sum_{\substack{j \in \Gamma(i) \\ |\bar{e}_{ij} \neq 0}} (e_{ij}^{\mathcal{M}})^{-1}$.

We note that each $e_{ij}^{\mathcal{M}}$ is positive and therefore so is D_i . This implies:

$$D_i = \sum_{j \in \Gamma(i)} (\mathcal{M} \bar{e}_{ij}^{-\frac{1}{2}} |\mathbf{x}_{ij}| \mathbf{x}_{ij}, \bar{e}_{ij}^{-\frac{1}{2}} |\mathbf{x}_{ij}| \mathbf{x}_{ij}) = \mathcal{M} : \sum_{j \in \Gamma(i)} \bar{e}_{ij}^{-\frac{1}{2}} |\mathbf{x}_{ij}| \mathbf{x}_{ij} \otimes \bar{e}_{ij}^{-\frac{1}{2}} |\mathbf{x}_{ij}| \mathbf{x}_{ij}.$$

Now, remembering that $A : B = \text{tr}({}^t A \cdot B)$, it is interesting to choose (among other solutions):

$$\mathcal{M}^i = \frac{D_i}{\dim} \left(\sum_{j \in \Gamma(i)} \bar{e}_{ij}^{-1} |\mathbf{x}_{ij}|^{-2} \mathbf{x}_{ij} \otimes \mathbf{x}_{ij} \right)^{-1} \Rightarrow \mathcal{M}_0^i = (\det(\mathcal{M}^i))^{-\frac{1}{2}} \mathcal{M}^i. \quad (6)$$

Global optimal metric (1)

The global optimal metric will be obtained by multiplying the pointwise metric by a scalar field to be determined:

$$\mathcal{M}_{opt}^i = C_i \mathcal{M}_0^i.$$

We search $(C_i)_i$ which minimizes

$$err_{L^1} = \sum_i meas_{\mathbf{x}}(i) \Gamma(i)^{-1} \sum_{\mathbf{x}_{ij}} (\mathbf{x}_{ij})^2 (\mathbf{x}_{ij}, C_i \mathcal{M}_0^i \mathbf{x}_{ij})^{-1} \bar{e}_{ij}$$

or

$$err_{L^1} = \sum_i \alpha_i C_i^{-1} ; \text{ with } \alpha_i = meas_{\mathbf{x}}(i) \Gamma(i)^{-1} \sum_{\mathbf{x}_{ij}} (\mathbf{x}_{ij})^2 (\mathbf{x}_{ij}, \mathcal{M}_0^i \mathbf{x}_{ij})^{-1} \bar{e}_{ij}$$

while satisfying to the constraint: $\sum_i meas_{\mathbf{x}}(i) \sqrt{\det(C_i \mathcal{M}_0^i)} = N$ or:

$$\sum_i \mu_i C_i^{\frac{dim}{2}} = N \text{ with } \mu_i = meas_{\mathbf{x}}(i) \sqrt{\det(\mathcal{M}_0^i)}.$$

Global optimal metric (2)

This can be simply solved by applying the variable change $d_i = \mu_i C_i^{\frac{dim}{2}}$, which gives:

$$\text{Min } \sum_i \eta_i d_i^{\frac{-2}{dim}} \text{ under the constraint } \sum_i d_i = N, \quad (7)$$

with $\eta_i = \alpha_i \mu_i^{\frac{2}{dim}}$. The solution of (7) writes:

$$d_i = \left(\sum_j \eta_j^{\frac{dim}{2+dim}} \right)^{-1} \eta_i^{\frac{dim}{2+dim}} N.$$

Global optimal metric (3)

Lemma: *The optimal metric is defined by:*

$$\mathcal{M}^i = C_i \mathcal{M}_0^i$$

with

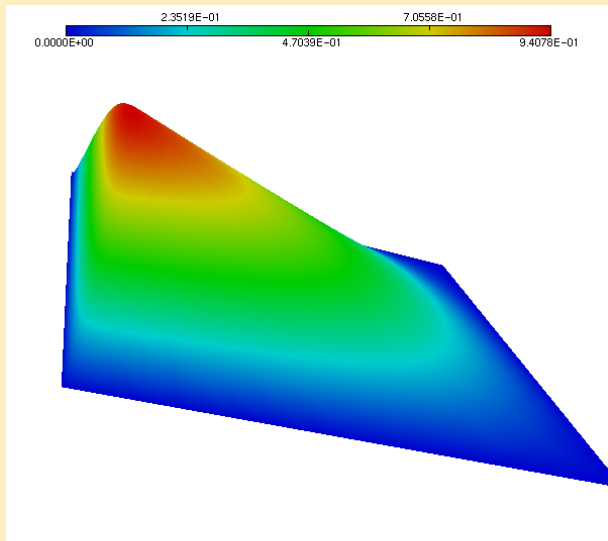
$$\mathcal{M}_0^i = (\det(\mathcal{M}_1^i))^{-\frac{1}{2}} \mathcal{M}_1^i, \quad \mathcal{M}_1^i = \frac{1}{\dim} \left(\sum_{j \in \Gamma(i)} \bar{e}_{ij}^{-1} |\mathbf{x}_{ij}|^{-2} \mathbf{x}_{ij} \otimes \mathbf{x}_{ij} \right)^{-1},$$

$$C_i = \mu_i^{-\frac{2}{\dim}} \left(\sum_j \eta_j^{\frac{\dim}{2+\dim}} \right)^{-\frac{2}{\dim}} \eta_i^{\frac{2}{2+\dim}} N^{\frac{2}{\dim}},$$

$$\eta_i = \alpha_i \mu_i^{\frac{2}{\dim}} ; \quad \alpha_i = \frac{\text{meas}_{\mathbf{x}}(i)}{\Gamma(i)} \sum_{\mathbf{x}_{ij}} \frac{(\mathbf{x}_{ij})^2}{(\mathbf{x}_{ij}, \mathcal{M}_0^i \mathbf{x}_{ij})} \bar{e}_{ij} ; \quad \mu_i = \text{meas}_{\mathbf{x}}(i) \sqrt{\det(\mathcal{M}_0^i)}. \square$$

Numerics (1)

A 2D boundary layer test case (Formaggia-Perrotto)



Numerics (1)

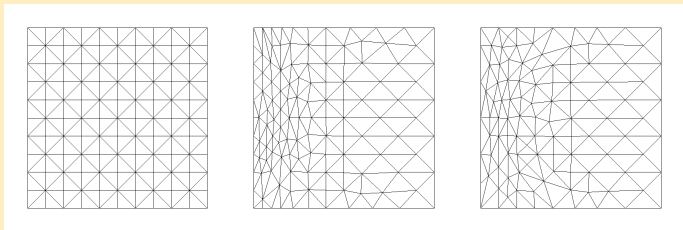


Figure : 2D boundary layer test case: initial uniform mesh (left), adapted mesh obtained by continuous Hessian-based adaptation (center) and tensorial Hessian-based adaptation (right).

Numerics (1)

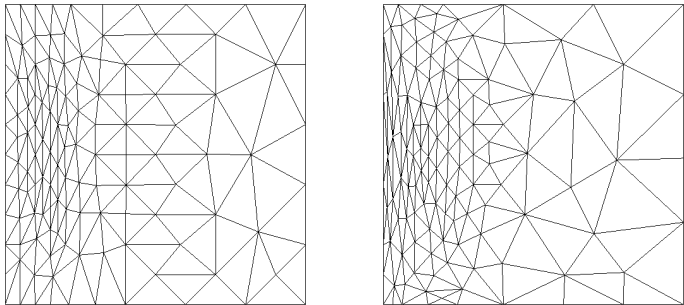


Figure : 2D boundary layer test case: adapted mesh obtained with continuous norm-oriented adaptation (left) and tensorial norm-oriented adaptation (right).

Numerics (1)

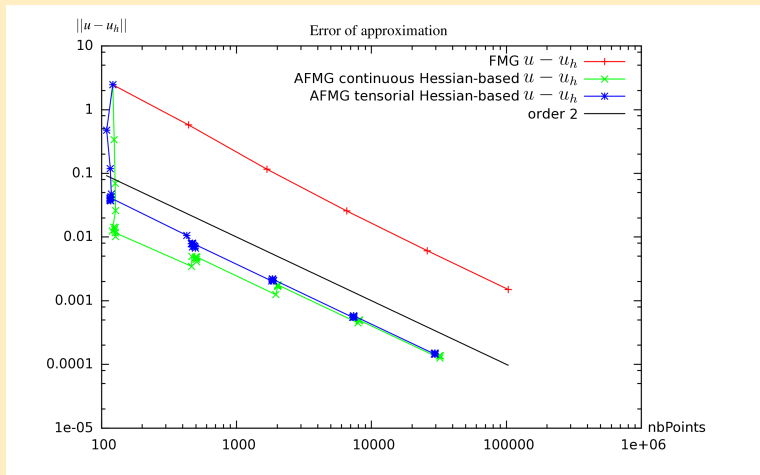


Figure : 2D boundary layer test case, Hessian-based methods: error convergence in terms of number of vertices.

Numerics (1)

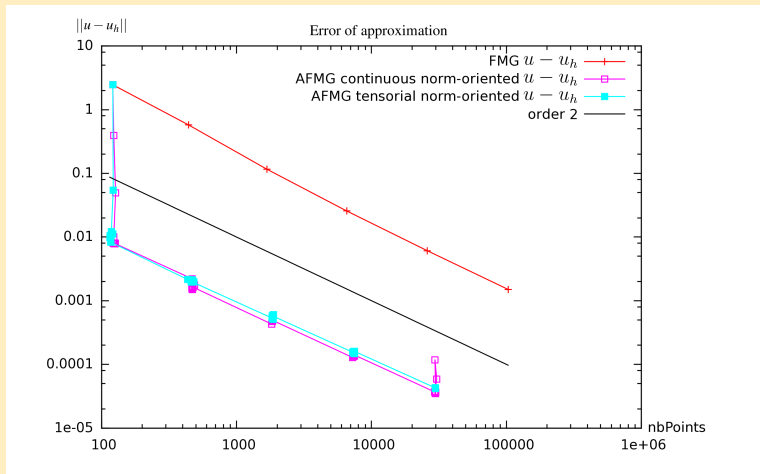


Figure : 2D boundary layer test case, norm-oriented methods: error convergence in terms of number of vertices.

Numerics (2)

The source term is a smooth Dirac derivative.

$$u(x, y) = \frac{1}{2} + \frac{1}{2} \sin\left(\frac{\pi\psi}{\varepsilon}\right)$$

$$\text{with } \psi = 0.25 - \sqrt{(x_C - x)^2 + (y_C - y)^2}.$$

$$\varepsilon = 0.02.$$

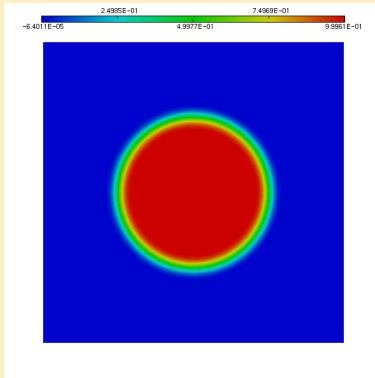


Figure : Circular-test-case-domain: sketch of the solution u .

Numerics (2)

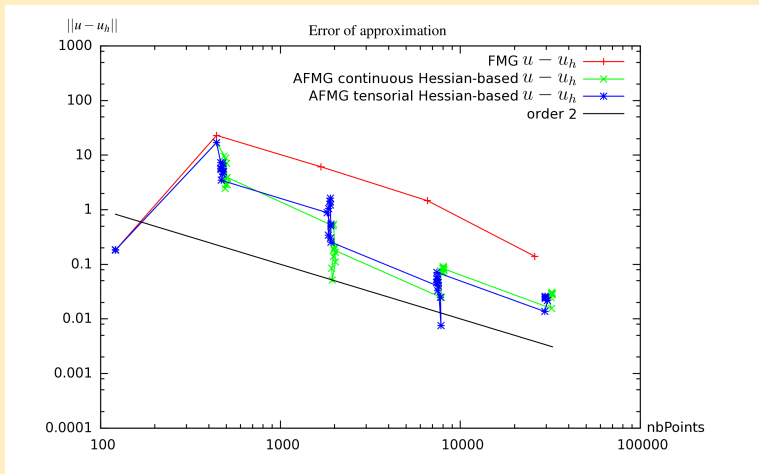


Figure : Bubble-like test case with thin interface, Hessian-based methods: error convergence in terms of number of vertices.

Numerics (2)

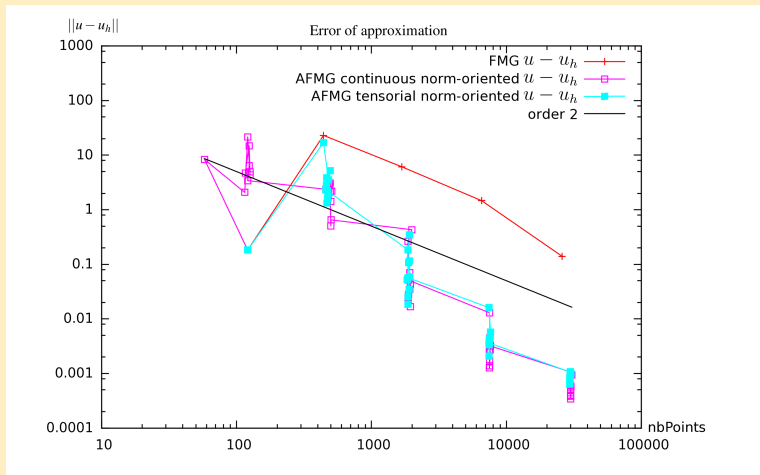
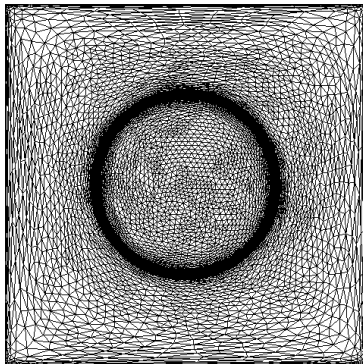
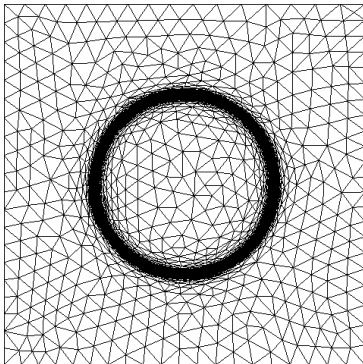


Figure : Bubble-like test case with thin interface, norm-oriented methods: error convergence in terms of number of vertices.

Numerics (2)



Numerics (2)

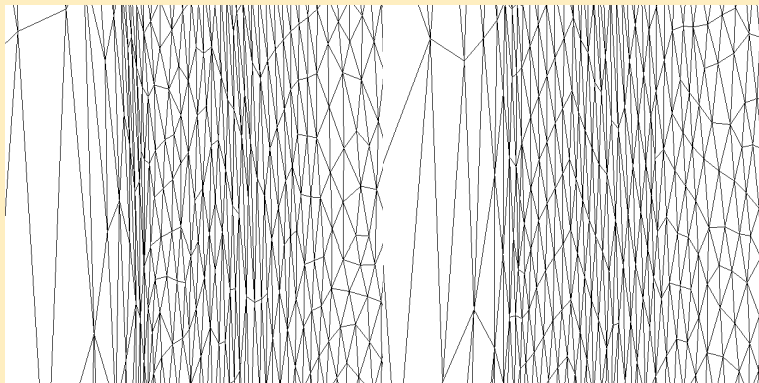
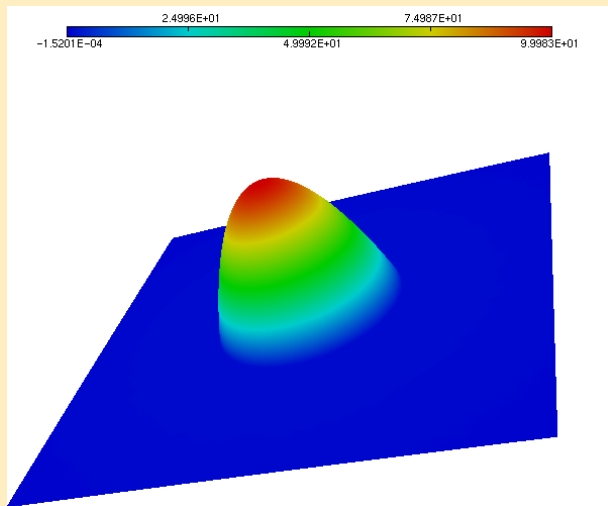


Figure : Bubble-like test case with thin interface, norm-oriented methods, sketch of meshes: top, global view of continuous option, left and tensorial option, right. Bottom, zooms near the point of discontinuity of maximal abscissa, of continuous option (left) and tensorial option (right).

Numerics (3)



Numerics (3)

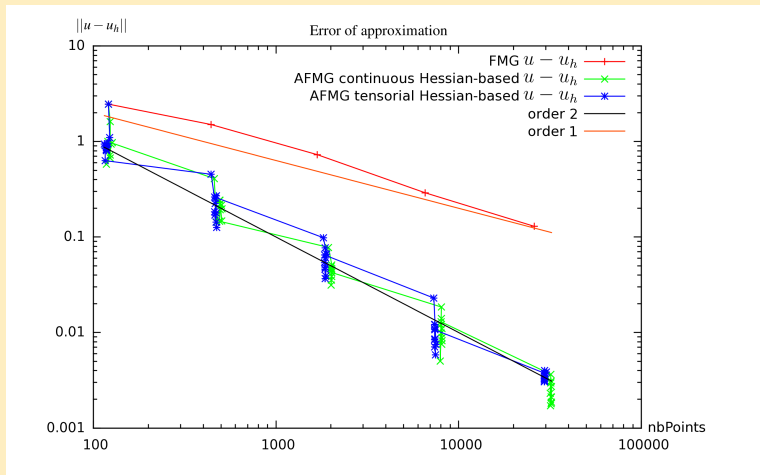


Figure : Poisson problem with discontinuous coefficient, Hessian-based methods: error convergence in terms of number of vertices.

Numerics (3)

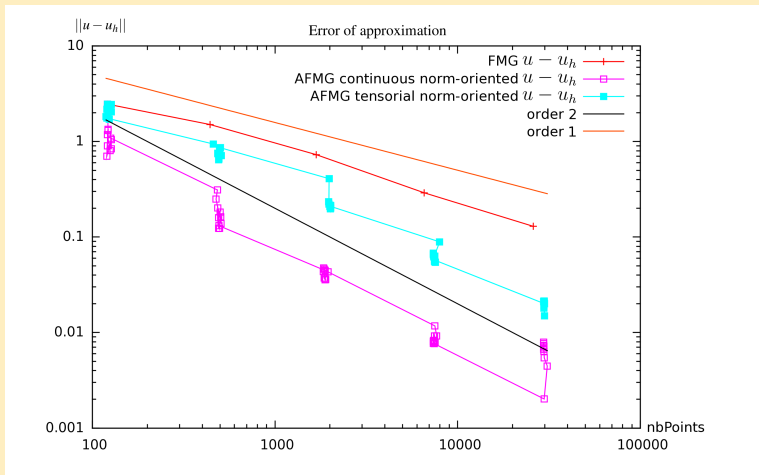
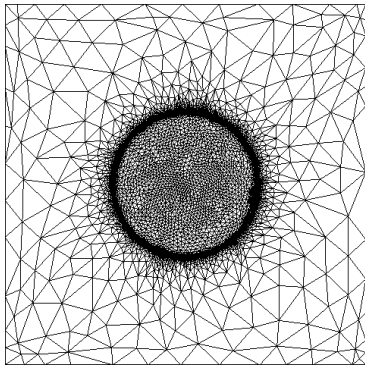
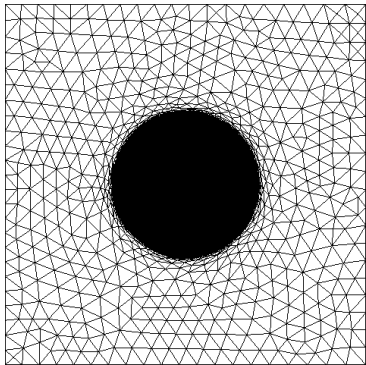


Figure : Poisson problem with discontinuous coefficient, norm-oriented methods: error convergence in terms of number of vertices.

Numerics (3)



Numerics (3)

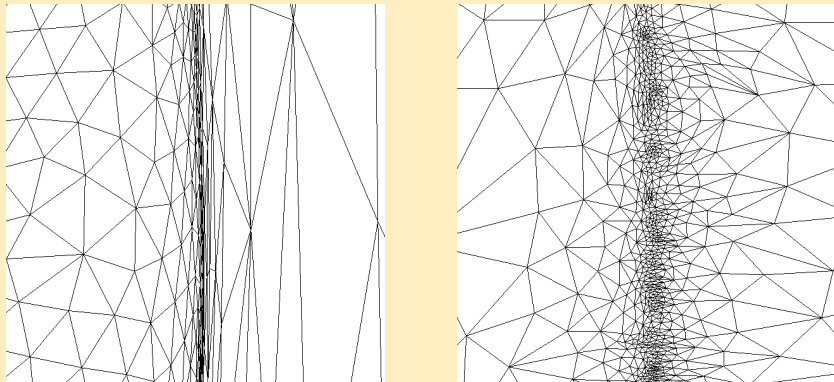


Figure : Poisson problem with discontinuous coefficient, sketch of meshes: top, global views of continuous option, left and tensorial option, right. Bottom, zooms near the point of discontinuity of maximal abscissa, of continuous norm oriented option (left) and tensorial norm oriented option, right.

Numerics (4)

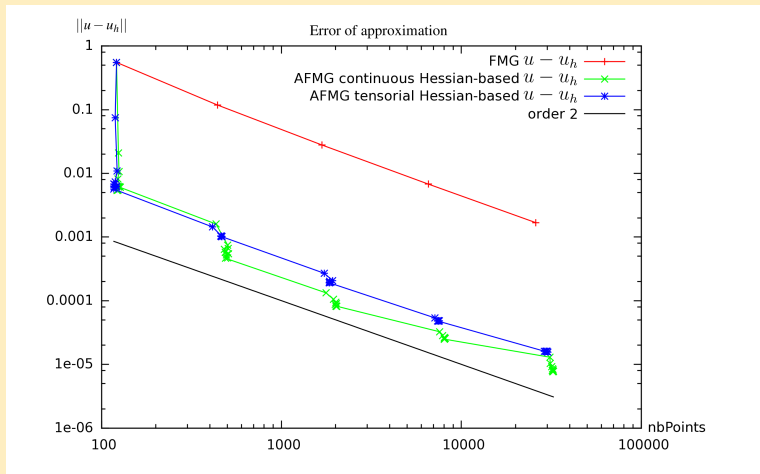


Figure : 1D boundary layer, Hessian-based methods: error convergence in terms of number of vertices.

Numerics (4)

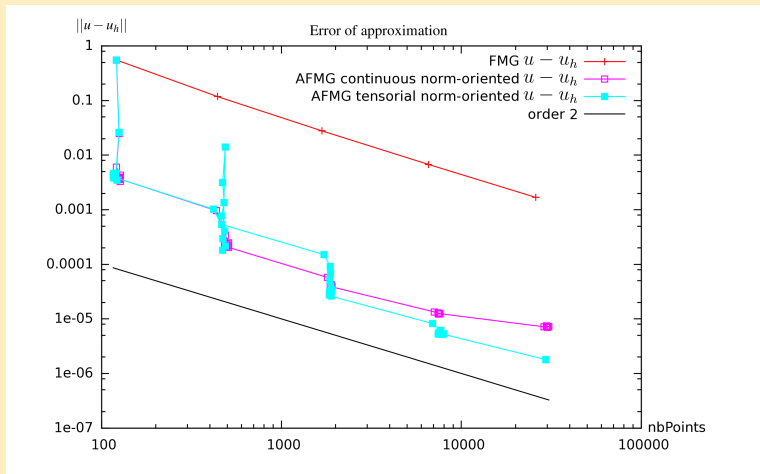


Figure : 1D boundary layer, norm-oriented methods: error convergence in terms of number of vertices.

Synthesis

Les deux méthodes ont des comportements proches pour les trois types de critères.

L'estimation plus fine du tensorial n'entraîne pas de progrès en adaptation.

Le tensoriel a besoin d'être amélioré pour traiter des discontinuités à l'intérieur du domaine.

Le continu se comporte un peu moins bien au bord.

L'étude continue.